Phosphorylation of CLASP2 by GSK-3β regulates its interaction with IQGAP1, EB1 and microtubules

Takashi Watanabe[1,2,*], Jun Noritake[1,3,*], Mai Kakeno[1,4], Toshinori Matsui[1], Takumi Harada[1], Shujie Wang[1], Norimichi Itoh[1], Kazuhide Sato[1], Kenji Matsuzawa[1], Akihiro Iwamatsu[5], Niels Galjart[6] and Kozo Kaibuchi[1,4,‡]

[1]Department of Cell Pharmacology, Graduate School of Medicine, Nagoya University, 65 Tsurumai, Showa, Nagoya, Aichi 466-8550, Japan
[2]Institute for Advanced Research, Nagoya University, Furo, Chikusa, Nagoya, Aichi 464-8601, Japan
[3]Department of Cell Physiology, Division of Membrane Physiology, National Institute for Physiological Sciences, Myodaiji, Okazaki, Aichi 444-8585, Japan
[4]JST, CREST, 4-1-8 Honcho, Kawaguchi 332-0012, Japan
[5]Protein Research Network, 1-13-5 Fukuura, Kanazawa, Yokohama, Kanagawa 236-0004, Japan
[6]Department of Cell Biology and Genetics, Erasmus MC, 3000 DR Rotterdam, Netherlands

*These authors contributed equally to this work
‡Author for correspondence (kaibuchi@med.nagoya-u.ac.jp)

Accepted 14 May 2009
Journal of Cell Science 122, 2969-2979 Published by The Company of Biologists 2009
doi:10.1242/jcs.046649

Summary

Polarised cell migration is required for various cell behaviours and functions. Actin and microtubules are coupled structurally and distributed asymmetrically along the front-rear axis of migrating cells. CLIP-associating proteins (CLASPs) accumulate near the ends of microtubules at the front of migrating cells to control microtubule dynamics and cytoskeletal coupling. Regional inhibition of GSK-3β is responsible for this asymmetric distribution of CLASPs. However, it is not known how GSK-3β regulates the activity of CLASPs for linkage between actin and microtubules. Here we identified IQGAP1, an actin-binding protein, as a novel CLASP-binding protein. GSK-3β directly phosphorylates CLASP2 at Ser533 and Ser537 within the region responsible for the IQGAP1 binding. Phosphorylation of CLASP2 results in the dissociation of CLASP2 from IQGAP1, EB1 and microtubules. At the leading edges of migrating fibroblasts, CLASP2 near microtubule ends partially colocalises with IQGAP1. Expression of active GSK-3β abrogates the distribution of CLASP2 on microtubules, but not that of a nonphosphorylatable CLASP2 mutant. The phosphorylated CLASP2 does not accumulate near the ends of microtubules at the leading edges. Thus, phosphorylation of CLASP2 by GSK-3β appears to control the regional linkage of microtubules to actin filaments through IQGAP1 for cell migration.

Supplementary material available online at
http://jcs.biologists.org/cgi/content/full/122/16/2969/DC1

Key words: GSK-3, IQGAP1, CLASP2, EB1, Microtubule

Introduction

Directional cell migration is necessary for developmental morphogenesis, tissue repair and tumour metastasis. A typical migrating cell has front-rear polarity with a single leading edge at the front end and a tail at the rear end. Cell polarisation includes the asymmetrical distribution of signalling molecules and cytoskeletal components, including actin filaments and microtubules (Ridley et al., 2003). Although actin and microtubules have distinct roles, these two cytoskeletal components are coordinated in a structural or regulatory manner during cell migration (Rodriguez et al., 2003; Watanabe et al., 2005). Among many regulatory molecules for cell migration, the Rho-family GTPases, including Rac1, Cdc42 and RhoA, have crucial roles in cell polarisation and migration through the regulation of actin filaments, microtubules and the adhesion apparatus (Burridge and Wennerberg, 2004; Fukata et al., 2003; Jaffe and Hall, 2005).

During the establishment of polarity in migrating cells, the temporal capture and stabilisation of some microtubule plus-ends occur near the actin-enriched leading edges, which are thought to enable the reorientation of the microtubule-organising centre and the Golgi complex toward the leading edges. These ensure that the cells exert biased vesicular transport for directional migration (Etienne-Manneville, 2004; Kirschner and Mitchison, 1986; Watanabe et al., 2005). Plus-end-tracking proteins (+TIPs) bind specifically to the growing ends of microtubules and affect microtubule dynamics (Akhmanova and Steinmetz, 2008). +TIPs include structurally unrelated protein families and are thought to connect the Rho-family GTPases to microtubules for the temporal stabilisation of microtubules, and for the coupling of microtubules to actin filaments (Gundersen et al., 2004; Watanabe et al., 2005). For example, activated Rac1/Cdc42 appears to interact with CLIP-170 (official symbol, CLIP1) through IQGAP1, an effector of Rac1/Cdc42 and an actin-binding protein, at the leading edges (Fukata et al., 2002; Watanabe et al., 2004). Although the Rho-family GTPases and their effectors show asymmetrical distribution and activity along the front-rear axis of migrating cells, the typical +TIPs such as EB1 and CLIP-170 accumulate uniformly at the growing ends of microtubules (Akhmanova and Steinmetz, 2008). Among the +TIPs, adenomatous polyposis coli (APC) and CLASPs accumulate asymmetrically in a population of the growing ends of microtubules near the cortex (Akhmanova et al., 2001; Bienz, 2002; Mimori-Kiyosue et al., 2005; Nathke et al., 1996; Watanabe et al., 2004; Reilein and Nelson, 2005; Wittmann and Waterman-Storer, 2005). Thus, they are probably involved in a region-specific control of microtubules in migrating cells.

Glycogen synthase kinase (GSK)-3 affects polarised cell migration through several microtubule-associated proteins, including +TIPs, such as APC and CLASPs. Phosphorylation of APC by GSK-3β abrogates its association with microtubules (Zumbrunn et al., 2001). Near the leading edges where GSK-3β is inactivated, nonphosphorylated APC appears to preferentially accumulate at the growing ends of microtubules, and it appears to be involved in regional control of microtubules (Etienne-Manneville and Hall, 2003). CLASPs were originally identified as CLIP-170-interacting proteins and later found to be required for microtubule stabilisation at the cortical regions of epithelial cells (Akhmanova et al., 2001; Mimori-Kiyosue et al., 2005). GSK-3β spatially regulates the binding of CLASPs to microtubules downstream of Rac1 (Akhmanova et al., 2001; Wittmann and Waterman-Storer, 2005). However, the regulatory mechanism of CLASPs by GSK-3β is poorly understood because of the lack of extensive in vitro studies.

In light of these observations, we searched for CLASP-interacting proteins to explore their functions. We identified IQGAP1, an actin-binding protein, as a novel CLASP-binding protein. Furthermore, we found that GSK-3β phosphorylated CLASP2 both in vitro and in vivo, and that this phosphorylation of CLASP2 inhibited its interaction with IQGAP1, EB1 and microtubules. Thus, GSK-3β appears to modulate the binding activity of CLASPs to microtubules and IQGAP1 at specified areas for coupling of microtubules to actin filaments in migrating cells.

Results

IQGAP1 is a novel CLASP2-interacting protein

To identify CLASP2-interacting proteins, the cytosolic fraction from porcine brain was applied to affinity beads coated with glutathione S-transferase (GST) alone, GST-CLASP2-N1 (residues 1-309), GST-CLASP2-N2 (310-670), GST-CLASP2-M (591-1016) or GST-CLASP2-C (1017-1294) (Fig. 1A). The bound proteins were eluted from the column and then resolved by SDS-PAGE. Several proteins with molecular masses of about 400 kDa (p400), 300 kDa (p300), 190 kDa (p190), 130 kDa (p130), 95 kDa (p95), 85 kDa (p85) and 82 kDa (p82) were specifically detected in the eluate from the GST-CLASP2-N2 affinity column (Fig. 1B). A protein with a molecular mass of ~170 kDa (p170) was observed in the eluate from the GST-CLASP2-C affinity column. No major proteins other than the GST or its fusion proteins were observed in the eluate from the GST (Fig. 1B), GST-CLASP2-N1 or GST-CLASP2-M affinity columns (data not shown). Since the C-terminal region of CLASP2 is known to interact with CLIP-170, which has a molecular mass of 170 kDa (Akhmanova et al., 2001), we examined whether p170 was CLIP-170. An antibody against CLIP-170 recognised p170, indicating that p170 was indeed CLIP-170 (Fig. 1C). By mass spectrometric analyses, p300, p190, p95, p85 and p82 were identified as FAM, IQGAP1, importin β1, phosphofructokinase and muscle-type phosphofructokinase, respectively. An antibody against IQGAP1 recognised p190 (Fig. 1C). Since IQGAP1 is involved in microtubule regulation downstream of Rac1 and Cdc42 (Fukata et al., 2002; Watanabe et al., 2004), we thereafter focused our investigation on IQGAP1.

CLASPs form a complex with IQGAP1

To examine whether CLASPs interact with IQGAP1 under physiological conditions, we first tried to precipitate CLASPs from the lysates of Vero fibroblasts. IQGAP1 was detected in the immunoprecipitates of two anti-CLASP2 antibodies (Fig. 2A). The

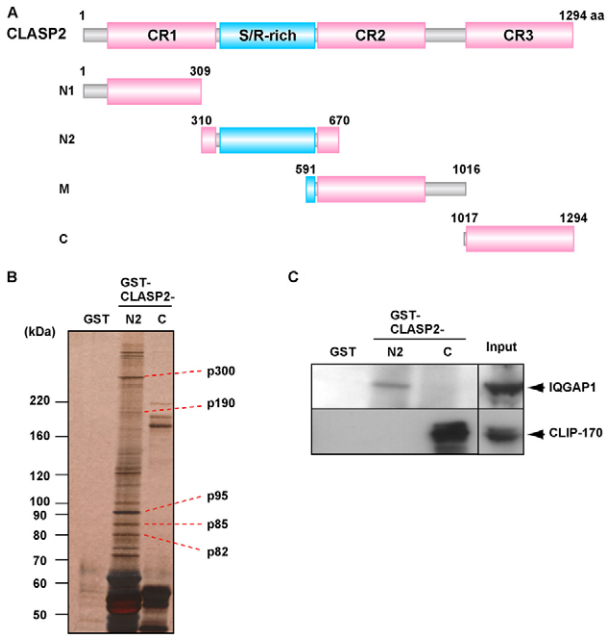

Fig. 1. Identification of IQGAP1 as a novel interacting molecule with CLASP2. (A) Schematic of CLASP2. The domain structures of CLASP2 and its various fragments are represented. CR, conserved region; S/R-rich, serine/arginine-rich. (B) The cytoplasmic fraction of porcine brain homogenates was loaded onto beads coated with GST, GST-CLASP2-N-terminal (GST-CLASP2-N2), or GST-CLASP2-C-terminal (GST-CLASP2-C) fragment. Aliquots of the eluate were resolved by SDS-PAGE, followed by silver staining (B) or immunoblotting with anti-IQGAP1 and anti-CLIP-170 antibodies (C). The identified bands are indicated according to their approximate molecular masses. All results are representative of three independent experiments.

recovery of IQGAP1 in the precipitates was approximately 3%. The broad reactive bands of CLASP2 might represent other isoforms and/or its phosphorylation (see below). We also expressed enhanced GFP (EGFP)-tagged CLASP1α, CLASP2α, and CLASP2γ in COS7 cells. When immunoprecipitated with an anti-GFP antibody, endogenous IQGAP1 was coprecipitated with all CLASP constructs (Fig. 2B). To determine the binding region of CLASP2 to IQGAP1, the indicated fragments of CLASP2 were fused to EGFP (Fig. 1A) and expressed in COS7 cells, followed by immunoprecipitation. Endogenous IQGAP1 was specifically coprecipitated with EGFP-CLASP2-N2, but not with the other constructs (Fig. 2C), indicating that the serine/arginine-rich region of CLASP2 is responsible for its interaction with IQGAP1. CLIP-170 was exclusively precipitated with EGFP-CLASP2-C (data not shown).

CLASP2 interacts directly with IQGAP1

To examine whether CLASP2 interacts directly with IQGAP1, we attempted an in vitro binding assay. Maltose-binding protein (MBP)-fused IQGAP1 fragments were produced, purified (Fig. 3A), and loaded onto affinity beads coated with GST-CLASP2-N2, because the serine/arginine-rich region of CLASP2 is sufficient for interaction with IQGAP1 (Fig. 2C). GST-CLASP2-N2 specifically interacted with MBP-IQGAP1-C (residues 746-1657) and MBP-IQGAP1-CT (1503-1657), but not with MBP, MBP-IQGAP1-N (1-863), or MBP-IQGAP1-GRD (998-1271) (Fig. 3B). Since IQGAP1-CT also binds to CLIP-170 (Fukata et al., 2002), we constructed

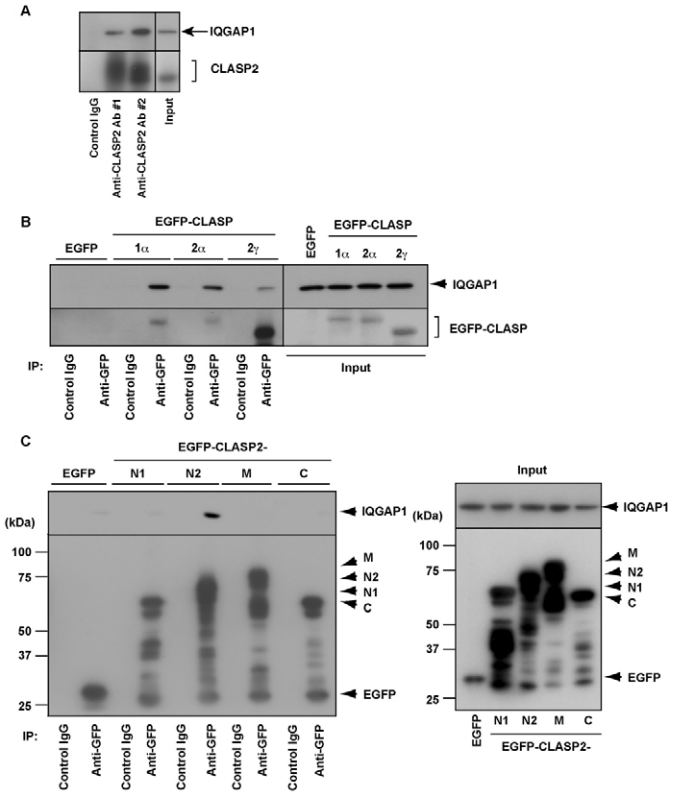

Fig. 2. Complex formation of CLASPs with IQGAP1. (A) The lysates from Vero cells were immunoprecipitated with two anti-CLASP2 antibodies. Endogenous IQGAP1 was precipitated with CLASP2. (B) The indicated EGFP-CLASP constructs were transfected into COS7 cells and immunoprecipitated with an anti-GFP antibody. IQGAP1 was coprecipitated with all examined EGFP-CLASPs (upper panel). (C) EGFP-CLASP2 fragments were transfected into COS7 cells and immunoprecipitated with an anti-GFP antibody. IQGAP1 was coprecipitated with EGFP-CLASP2-N2. The expression levels of the different CLASP2 fragments are similar. All results are representative of three independent experiments.

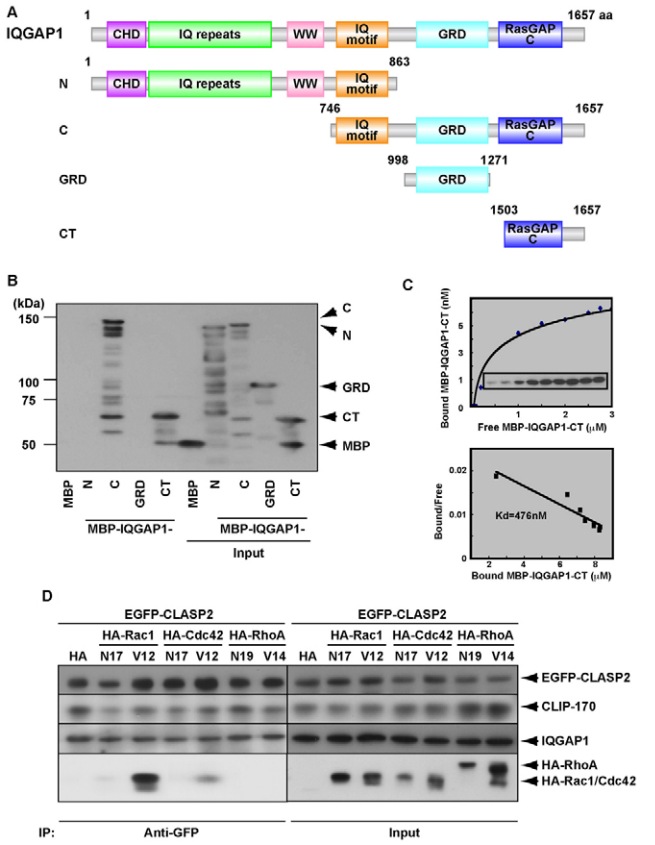

Fig. 3. Direct interaction of CLASP2 with IQGAP1. (A) Schematic of IQGAP1. The domain structures of IQGAP1 and its various fragments are represented. CHD, calponin homology domain; GRD, Ras-GAP-related domain; IQ motif, calmodulin-binding motif; IQ repeats, IQGAP-specific repeat motif. (B) Purified MBP-fused IQGAP1 fragments were mixed with the affinity beads coated with purified GST-CLASP2-N2. Bound MBP fusion proteins were coeluted with GST fusion proteins by glutathione. The eluates were subjected to SDS-PAGE, followed by immunoblotting with an anti-MBP antibody. The bands lower than MBP-IQGAP1-C in the input represent the degradation products of MBP-IQGAP1-C, which lacks the C-terminus of IQGAP1. (C) Saturable interaction of purified GST-CLASP2-N2 with MBP-IQGAP1-CT. The indicated concentrations of MBP-IQGAP1-CT were incubated with the beads coated with GST-CLASP2-N2 (100 pmol), and the K_d value was calculated by Scatchard analysis. (D) EGFP-CLASP2 and indicated HA-tagged small GTPases were transfected into COS7 cells. HA-Rac1^{V12} and HA-Cdc42^{V12} were coprecipitated with EGFP-CLASP2 and IQGAP1, whereas HA-Rac1^{N17}, HA-Cdc42^{N17}, HA-RhoA^{N19}, and HA-RhoA^{V14} were not. All results are representative of three independent experiments.

additional deletion fragments and performed in vitro binding assays. However, we could not distinguish between the CLASP2-binding region and the CLIP-170-binding region (data not shown). The binding of MBP-IQGAP1-CT to GST-CLASP2-N2 was dose-dependent and saturable (Fig. 3C). Scatchard analysis revealed a single class of affinity binding sites with a K_d of about 480 nM. Taken together, these results indicate that IQGAP1-CT binds directly to CLASP2-N2.

Rac1/Cdc42, IQGAP1 and CLASP2 form a complex

Since IQGAP1 is an effector of Rac1 and Cdc42 (Hart et al., 1996; Kuroda et al., 1996; McCallum et al., 1996), we examined whether Rac1/Cdc42, IQGAP1 and CLASP2 form a complex. When EGFP-CLASP2 was immunoprecipitated from the cells expressing EGFP-CLASP2 and constitutively active Rac1 (Rac1^{V12}), Rac1^{V12} and IQGAP1 were coimmunoprecipitated (Fig. 3D). Similar results were obtained with constitutively active Cdc42 (Cdc42^{V12}) instead of Rac1^{V12}. Constitutively active RhoA (RhoA^{V14}), dominant-negative Rac1 (Rac1^{N17}), dominant-negative Cdc42 (Cdc42^{N17}) and dominant-negative RhoA (RhoA^{N19}) were not coimmunoprecipitated with EGFP-CLASP2. Under these conditions, CLIP-170 was also precipitated, possibly by its direct association with CLASP2 and/or through IQGAP1. These results suggest that activated Rac1/Cdc42, IQGAP1 and CLASP2 can form a complex. The Rho-family GTPases did not significantly affect the coprecipitation of CLIP-170 or IQGAP1.

GSK-3β phosphorylates CLASP2 at Ser533 and Ser537

GSK-3β can phosphorylate CLASP2 in vitro, and the inhibition of GSK-3β in epithelial cells impairs the mobility shift of CLASP2 (Wittmann and Waterman-Storer, 2005). Although many putative consensus sites for phosphorylation by GSK-3β [Ser/Thr-x-x-x-Ser/Thr (Cohen and Frame, 2001)] are found in CLASP2, especially in the serine/arginine-rich region, the specific phosphorylation sites in CLASP2 have not yet been identified.

To examine the phosphorylation of CLASP2 in vivo, EGFP-CLASP2-N2 was transfected into COS7 cells with wild-type (WT), kinase-inactive (KN) or constitutively active (S9A) forms of GSK-3β and then subjected to SDS-PAGE. The fast and slow migrating bands of EGFP-CLASP2-N2 were observed without GSK-3β. In cells expressing GSK-3β WT or S9A, only a slowly migrating band was evident (Fig. 4A). When the cells were treated with GSK-3 inhibitors (SB216763 and SB415286), the mobility shift of CLASP2 was partially abrogated (Fig. 4B). The mobility shifts were more evident in 2D-PAGE (supplementary material Fig. S1). Taken together, our results indicate that CLASP2-N2 is phosphorylated by GSK-3β in vivo. Except for the serine/arginine-rich region (N2), no significant mobility shift of other CLASP2 fragments was observed in SDS-PAGE (data not shown).

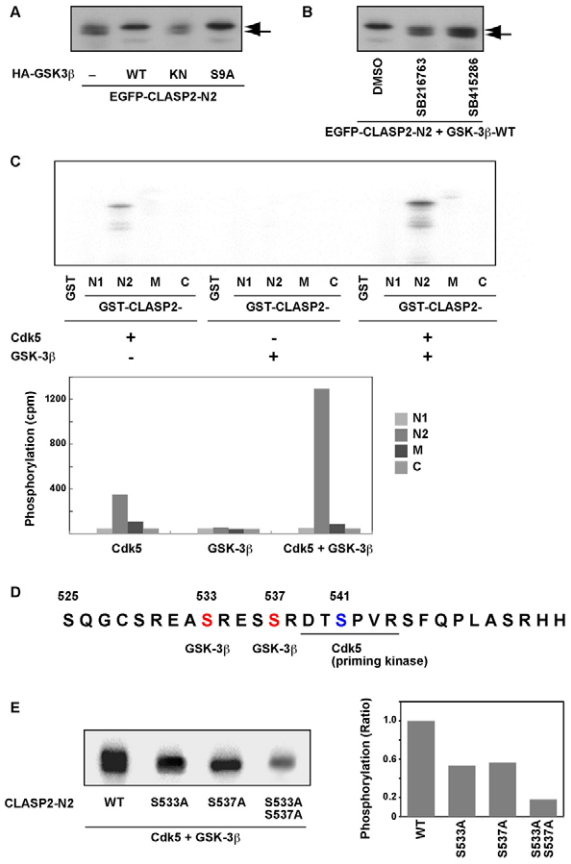

Fig. 4. Phosphorylation of CLASP2 at Ser533 and Ser537 by GSK-3β. (A) COS7 cells were transfected with EGFP-CLASP2-N2 and the indicated GSK-3β construct. Each lysate was subjected to SDS-PAGE, followed by immunoblot with an anti-GFP antibody. The arrow and arrowhead indicate fast and slow migrating bands of EGFP-CLASP2-N2, respectively. (B) The cells expressing EGFP-CLASP2-N2 and GSK-3β WT were cultured in the presence of GSK-3 inhibitors (10 μM SB216763, 50 μM SB415286) or control vehicle (DMSO) for 1 hour. Each lysate was subjected to immunoblotting with an anti-GFP antibody. The arrow and arrowhead indicate fast and slow migrating bands of EGFP-CLASP2-N2, respectively. (C) A kinase assay was performed in vitro using purified GST-CLASP2-N2, GSK-3β and Cdk5. Each reaction mixture was subjected to SDS-PAGE and detected by autoradiography. Phosphorylation levels of CLASP2 fragments are shown in the bar graph. (D) Potential phosphorylation sites of GSK-3β and Cdk5. The numbers denote amino acid positions of CLASP2. The underlined residues represent a consensus motif recognised by Cdk5. (E) In vitro kinase assay was performed using purified CLASP2-N2 Ala-substituted mutants, GSK-3β and Cdk5. Each reaction mixture was subjected to SDS-PAGE and detected by autoradiography. The phosphorylation levels of CLASP2 WT or mutants are shown in the bar graph. All results are representative of three independent experiments.

Next, purified CLASP2 fragments (N1, N2, M and C) were used to examine whether GSK-3β directly phosphorylates CLASP2 in vitro. GSK-3β itself phosphorylated none of these fragments efficiently (Fig. 4C). GSK-3β generally requires prephosphorylation of its substrates by other kinases (Eldar-Finkelman, 2002). Since CLASP2 has several putative phosphorylation sites of protein kinase C (PKC), protein kinase A (PKA), cyclin-dependent kinase 5 (Cdk5), Jun N-terminal kinase (JNK), and casein kinase II (CKII), we performed in vitro phosphorylation assays with these kinases. Cdk5 phosphorylated the CLASP2-N2 fragment, but did not significantly phosphorylate other CLASP2 fragments (Fig. 4C). The other kinases did not phosphorylate any fragments of CLASP2 under the same conditions (data not shown). When both Cdk5 and GSK-3β were used simultaneously, the phosphorylation level of CLASP2 was significantly increased in comparison to when Cdk5 alone was used (Fig. 4C), suggesting that Cdk5 functions as a priming kinase, at least in a cell-free system.

CLASP2 has a consensus motif recognised by Cdk5 at Ser541 in the vicinity of the potential phosphorylation sites of GSK-3β, Ser533 and Ser537 (Fig. 4D). We produced nonphosphorylatable constructs of CLASP2-N2 named S533A and S537A, by converting Ser to Ala, and performed an in vitro phosphorylation assay to determine the phosphorylation site of CLASP2 by GSK-3β. These Ala-substituted mutants significantly reduced the phosphorylation level of CLASP2 (Fig. 4E). Furthermore, a nonphosphorylatable double mutant of S533 and S537 (2A) reduced the phosphorylation level more than either single Ala-substituted mutant S533A or S537A (Fig. 4E). Since the 2A mutant was still phosphorylated to a small extent in vitro, it appears that GSK-3β can phosphorylate other minor sites after Cdk5 phosphorylation.

Phosphorylation of CLASP2 inhibits its interaction with IQGAP1, EB1 and microtubules

We next examined whether the interaction of CLASP2 with IQGAP1 was affected by CLASP2 phosphorylation. When the fragment containing both the GSK-3β phosphorylation sites and the IQGAP1-binding region EGFP-CLASP2-N2 was transfected into COS7 cells, endogenous IQGAP1 was coimmunoprecipitated with EGFP-CLASP2-N2 (Fig. 5A). This interaction was decreased by cotransfection with GSK-3β WT or S9A, but not with KN (Fig. 5A). Similar results were obtained with the use of EGFP-CLASP2 (full-length) instead of the fragment (supplementary material Fig. S2A). Interestingly, the inhibitory effects of GSK-3β WT and S9A were more apparent in the cells expressing EGFP-CLASP2-N2 than in those expressing EGFP-CLASP2. This difference might be explained by more efficient phosphorylation of EGFP-CLASP2-N2 in COS7 cells. Treatment with GSK-3 inhibitors restored the inhibitory effect of GSK-3β WT (supplementary material Fig. S2B). In addition, inhibition of endogenous GSK-3 activity also increased the association between endogenous IQGAP1 and CLASP2 in Vero fibroblasts (supplementary material Fig. S2C). Of note, the GSK-3 inhibitors attenuated the efficiency of immunoprecipitation. One possible explanation is that the GSK-3 inhibitors induce the dephosphorylation of CLASP2 and change its conformational state, thereby preventing recognition by the antibodies used.

Since EB1 is known to interact with CLASPs and this interaction is necessary for the regulation of microtubule dynamics (Mimori-Kiyosue et al., 2005), we examined how it was affected by the

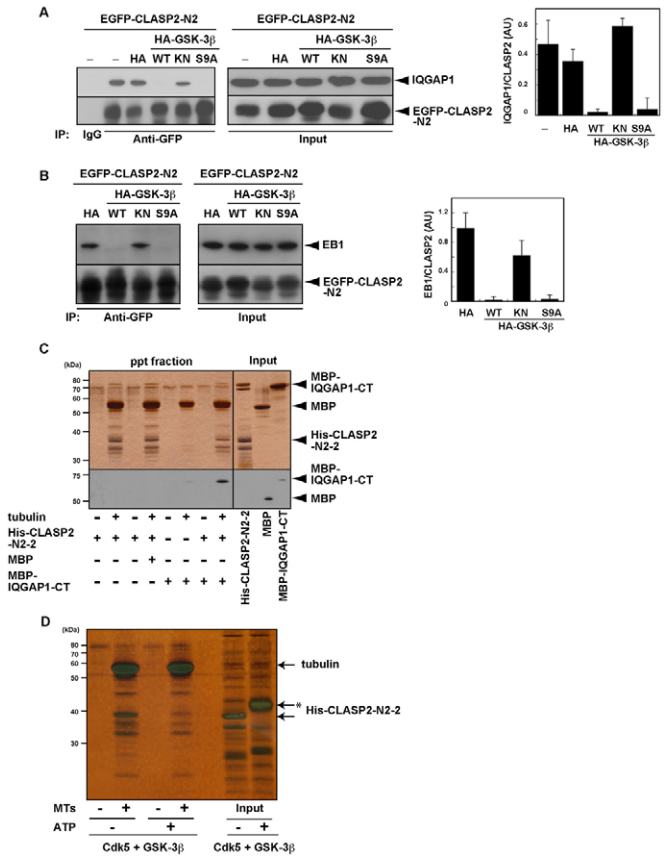

Fig. 5. Impaired association of phosphorylated CLASP2 with IQGAP1, EB1, and microtubules. (A) COS7 cells were transfected with EGFP-CLASP2-N2 and the indicated GSK-3β construct. When immunoprecipitated with an anti-GFP antibody, IQGAP1 was coprecipitated with EGFP-CLASP2-N2, whereas this interaction was abrogated in the presence of active GSK-3β. (B) EGFP-CLASP2-N2 and the indicated GSK-3β construct were transfected into COS7 cells, and immunoprecipitated with an anti-GFP antibody. EB1 was coimmunoprecipitated with EGFP-CLASP2-N2, whereas this association was inhibited by active GSK-3β. The ratio of the coprecipitates (mean ± s.d.) to precipitated CLASP2 is shown in the bar graph on the right. (C) Purified CLASP2-N2-2 (aa 263-581) and MBP-IQGAP1-CT were designed to examine their association with in vitro polymerised microtubules. His-CLASP2-N2-2 was sedimented in a microtubule-dependent manner. IQGAP1 was cosedimented with microtubules only in the presence of CLASP2. The upper and lower panels show the results of silver staining and immunoblotting with an anti-His antibody, respectively. (D) Phosphorylated His-CLASP2-N2-2 was not sedimented with microtubules. Phosphorylated His-CLASP2-N2-2 (asterisk) migrated more slowly than its nonphosphorylated form. All results are representative of more than three independent experiments.

phosphorylation of CLASP2. Endogenous EB1 was coimmunoprecipitated with EGFP-CLASP2-N2 from COS7 cells (Fig. 5B). This association was also inhibited in the presence of GSK-3β WT or S9A (Fig. 5B). Since IQGAP1 and EB1 bind to the same region within CLASP2, we performed a competition assay. Increasing amounts of purified EB1 did not appear to interfere with the association of MBP-IQGAP1-CT with GST-CLASP2-N2 (supplementary material Fig. S2D), indicating that EB1 and IQGAP1 are able to simultaneously associate with CLASP2.

We also examined the binding of CLASP2 to microtubules in vitro. Purified CLASP2-N2-2 (residues 263-581) was sedimented with microtubules (Fig. 5C). IQGAP1 was sedimented in the presence of CLASP2-N2-2, but not in the absence of CLASP2-N2-2 (Fig. 5C), suggesting that IQGAP1 binds to microtubules through CLASP2, and that CLASP2 can simultaneously bind to IQGAP1 and microtubules. Furthermore, the association of CLASP2 with microtubules was impaired after the phosphorylation by GSK-3β (Fig. 5D). Thus, GSK-3β can modulate the binding ability of CLASP2 to microtubules as well as to EB1 and IQGAP1.

To further examine the role of CLASP2 phosphorylation at Ser533 and Ser537 in the interaction with IQGAP1 and EB1, we used the nonphosphorylatable EGFP-CLASP2-N2 mutant (EGFP-CLASP2-N2-2A; EGFP-fused CLASP2-N2 harbouring two Ala substitutions at Ser533 and Ser537). In the presence of GSK-3β KN, both EGFP-CLASP2-N2 and EGFP-CLASP2-N2-2A associated with purified GST-IQGAP1-CT and GST-EB1 (Fig. 6A). The recovery to GST-EB1 was greater than that to GST-IQGAP1-CT, suggesting that CLASP2 binds to EB1 with a higher affinity. When GSK-3β WT was transfected, EGFP-CLASP2-N2 did not associate with either GST-IQGAP1-CT or GST-EB1, whereas EGFP-CLASP2-N2-2A did (Fig. 6A), suggesting that Ala substitutions at Ser533 and Ser537 can be resistant to the inhibitory effect of GSK-3β. We also attempted to produce a phosphomimic EGFP-CLASP2-N2 mutant, in which Ser533 and Ser537 were replaced by Asp or Glu, but found that these mutants still bound GST-IQGAP1-CT and GST-EB1 (data not shown), indicating that these substitutions cannot mimic the phosphorylation state and/or were not sufficient. Taken together, our results indicate that GSK-3β negatively regulates the interaction of CLASP2 with IQGAP1 and EB1 through the phosphorylation at Ser533 and Ser537.

CLASP2 distributes asymmetrically in migrating cells

To further understand the regulation of CLASP2 by GSK-3β, we examined the subcellular localisation of CLASP2 and IQGAP1 in Vero fibroblasts. IQGAP1 localised to the leading edges where microtubules were targeted (Fig. 6B), whereas CLASP2 accumulated near the plus-ends of a subset of microtubules toward the leading edges in Vero cells. Microtubule-associated CLASP2 partially colocalised with EB1 as well as microtubule lattices behind the EB1 signal (Fig. 6C), essentially as described previously (Akhmanova et al., 2001; Fukata et al., 2002; Wittmann and Waterman-Storer, 2005). IQGAP1 partially colocalised with CLASP2 at the leading edges (Fig. 6B). EB1 accumulated at the plus-ends of microtubules, not only near the leading edges, but also throughout the wider cortical region and central region; however, CLASP2 was distributed asymmetrically to the ends of microtubules (Mimori-Kiyosue et al., 2005; Wittmann and Waterman-Storer, 2005). Transfection of GSK-3β S9A induced the delocalisation of EGFP-CLASP2 both from microtubules (Wittmann and Waterman-Storer, 2005) and EB1 (Fig. 6C), which prevented partial colocalisation of CLASP2 with IQGAP1 at the leading edges (Fig. 6C). However, GSK-3β KN did not affect the localisation of CLASP2 significantly (supplementary material Fig. S3A). The inhibitory effect of GSK-3β S9A was negated by treatment of the cells with GSK-3 inhibitors (SB216763 and SB415286) (Fig. 6C; and data not shown), but not by treatment with the vehicle alone (supplementary material Fig. S3B). In fact, these inhibitors enhanced the accumulation of CLASP2 on microtubules. Furthermore, when endogenous GSK-3 was eliminated by RNAi, CLASP2 on microtubules was more apparent throughout the cells (supplementary material Fig. S3C,D), similarly to the cells treated with GSK-3 inhibitors. The effect of the depletion was moderate in the comparison with that of the inhibitors. This might be because

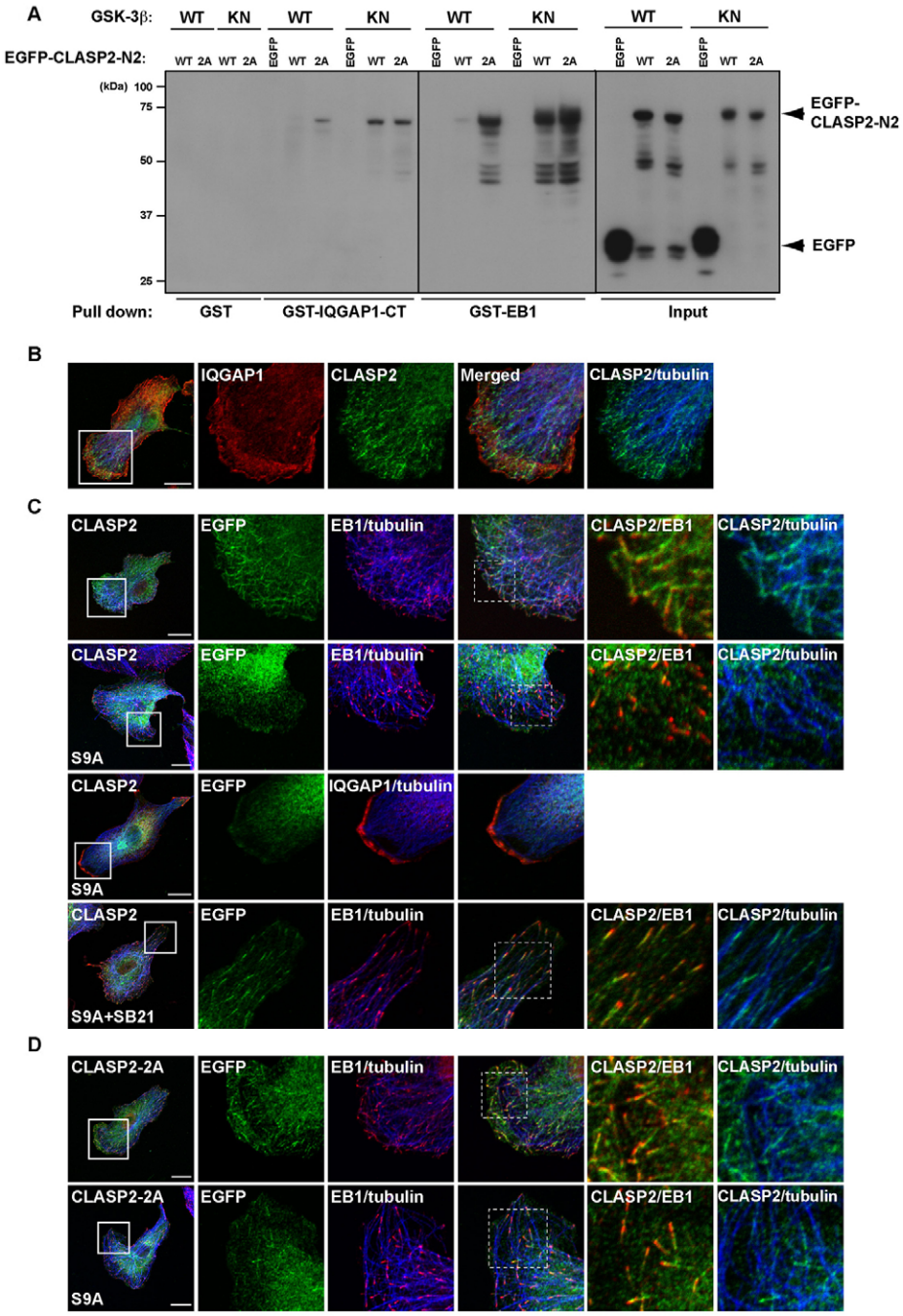

Fig. 6. Effect of GSK-3β on the distribution and binding of CLASP2. (A) EGFP-CLASP2-N2-WT or EGFP-CLASP2-N2-2A mutant was transfected into COS7 cells. The lysates were subjected to pull down with GST-IQGAP1-CT or GST-EB1. The 2A mutant was precipitated with GST-IQGAP1-CT or GST-EB1. The active GSK-3β WT inhibited the association of CLASP2-N2-WT, but not that of the CLASP2-N2-2A mutant, with IQGAP1 and EB1. (B) Vero cells were stained with anti-IQGAP1 (red) and anti-CLASP2 (green) antibodies. These images were merged with the staining of the anti-tubulin antibody (blue). (C) Vero cells transfected with EGFP-CLASP2 were stained with anti-EB1 or anti-IQGAP1, together with anti-tubulin antibodies (blue). Green represents EGFP-CLASP2 and red indicates EB1 or IQGAP1. Insets in panels are magnified in the right panels. Scale bars: 10 μm. (D) Vero cells were transfected with EGFP-CLASP2-2A, followed by immunostaining with anti-EB1 (red) and anti-tubulin (blue) antibodies. Insets in panels are magnified in the right panels. Scale bars: 10 μm. The cells cotransfected with GSK-3β S9A are indicated by S9A and those treated with the GSK-3 inhibitor SB216763 at 10 μM for 1 hour before fixation are labelled SB21. All results are representative of more than three independent experiments.

the depletion of GSK-3 was incomplete, and mechanisms in addition to GSK-3-mediated phosphorylation contributed to the regulation of CLASP2-microtubule association. The nonphosphorylatable mutant, EGFP-CLASP2-2A, showed a similar localisation with EGFP-CLASP2, whereas GSK-3β S9A had a lesser effect on EGFP-CLASP2-2A in comparison with the wild type (Fig. 6C,D). These observations, taken together with the in vitro results (Fig. 5C,D), indicate that GSK-3β impairs the localisation of CLASP2 along microtubules by phosphorylating CLASP2 at Ser533 and Ser537.

To further examine the role of CLASP2 phosphorylation by GSK-3β, we raised a rabbit polyclonal antibody that specifically recognises the phosphorylated CLASP2 at Ser533 and Ser537 (anti-S533/S537-*P* antibody). The specificity of this antibody was examined by immunoblot analysis (Fig. 7A). A fixed amount (2 pmol) of GST-CLASP2-N2 containing increasing amounts of the phosphorylated form was loaded on the gel. The anti-S533/S537-*P* antibody recognised the phosphorylated CLASP2 in a dose-dependent manner, indicating that the antibody specifically recognises the phosphorylated CLASP2 at Ser533 and Ser537. We next examined whether GSK-3β could phosphorylate CLASP2 at Ser533 and Ser537 in COS7 and Vero cells. Transfection of GSK-3β WT or S9A induced the phosphorylation of EGFP-CLASP2-N2 at Ser533 and Ser537, whereas the active GSK-3β failed to induce the phosphorylation of EGFP-CLASP2-N2-2A (Fig. 7B). Treatment of the cells with GSK-3 inhibitors partially abolished the GSK-3β-

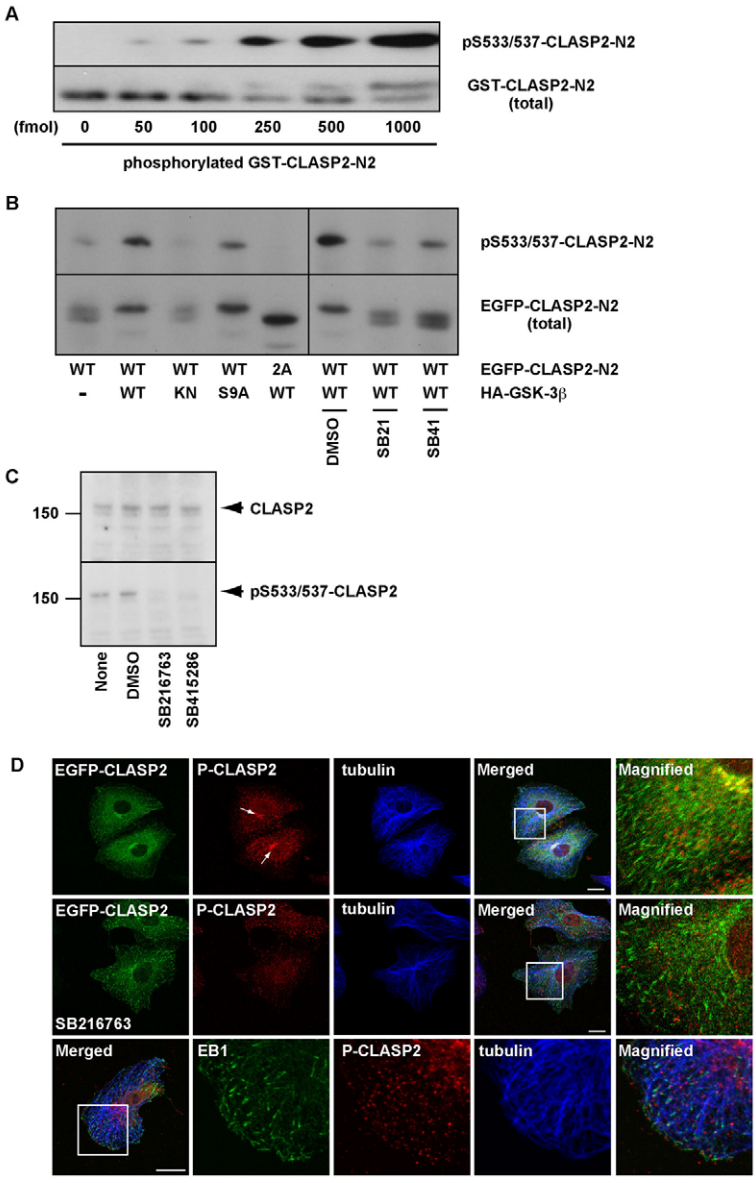

Fig. 7. Distribution of phosphorylated CLASP2 in cells. (A) Purified GST-CLASP2-N2 (2 pmol) containing the indicated amounts of GST-CLASP2-N2 phosphorylated by GSK-3β was subjected to SDS-PAGE, followed by immunoblot analysis with anti-S533/537-*P* (upper panel) or anti-GST antibodies (lower panel). (B) COS7 cells were transfected with EGFP-CLASP2-N2 and the indicated GSK-3β construct. In the right panels, the cells were treated with GSK-3 inhibitors (SB216763 and SB415286) or control vehicle (DMSO). Each lysate was subjected to SDS-PAGE and immunoblot analysis with anti-S533/S537-*P* (upper panel) and anti-GFP antibodies (lower panel). The same lysates were used in Fig. 4. (C) Vero cells were treated with DMSO, 10 μM SB216763 or 50 μM SB415286 for 1 hour. The lysates were blotted with an anti-CLASP2 (upper panel) and anti-S533/537-*P* antibodies (lower panel). (D) Vero cells expressing EGFP-CLASP2 were stained with an anti-S533/S537-*P* antibody (P-CLASP2; red). The immunoreactivity of this antibody did not show significant colocalisation with EGFP-CLAPS2 signals (green), except in the perinuclear region (arrow). The cells were treated with a GSK-3 inhibitor (10 μM SB216763) for 1 hour before fixation (middle row). The immunoreactivity of the anti-S533/537-*P* antibody (red) was compared with EB1 (green) and tubulin (blue) in the lowest row. Insets in merged images are magnified in the right panels. Scale bars: 10 μm. All results are representative of three independent experiments.

induced phosphorylation of EGFP-CLASP2-N2 in COS7 cells (Fig. 7B). The anti-S533/537-*P* antibody could recognise the phosphorylation of endogenous CLASP2 at Ser533 and Ser537 in Vero cells, and the immunoreactivity was also abrogated by treatment with GSK-3β inhibitors (Fig. 7C), indicating that CLASP2 is phosphorylated at Ser533 and Ser537 by GSK-3β under physiological conditions.

In Vero fibroblasts, the immunoreactivity of the anti-S533/S537-*P* antibody was mainly detected at the perinuclear region, where it colocalised with the fluorescence of EGFP-CLASP2 (Fig. 7D). Treatment with a GSK-3β inhibitor abolished the immunoreactivity at the perinuclear region. However, the GSK-3 inhibitor did not apparently affect the fine dot-like immunofluorescence. In addition, this immunofluorescence showed negligible colocalisation with the fluorescence of EGFP-CLASP2, especially at the leading edges (Fig. 7D). These results suggest that phosphorylated CLASP2 stays at the perinuclear region, but not on the ends and lattices of microtubules at the leading edges. However, we cannot exclude the possibility that with the exception of localisation in the perinuclear region, the immunofluorescence of the anti-S533/537-*P* antibody is background staining.

Finally, to examine the functional significance of the interaction between IQGAP1 and CLASP2 in cell migration, we used the Boyden chamber assay. Endogenous IQGAP1 or CLASP2 was depleted by two independent siRNAs (Fig. 8A). The transfection of each siRNA impaired the serum-stimulated cell motility from the upper to the basal membrane (Fig. 8B). The two siRNAs showed similar effects on cell motility. The inhibitory effect of siRNA to IQGAP1 was almost completely rescued by the expression of RNAi-resistant ($RNAi^R$)-full length IQGAP1, but not that of $RNAi^R$-IQGAP1-ΔCT lacking the CLASP2-binding region (Fig. 8B). This indicates that the linkage of CLASP2 to IQGAP1 is required for effective cell migration.

Taken together, these results suggest that GSK-3β dynamically and negatively regulates the binding of CLASP2 to EB1 and microtubules for asymmetrical distribution on microtubules by

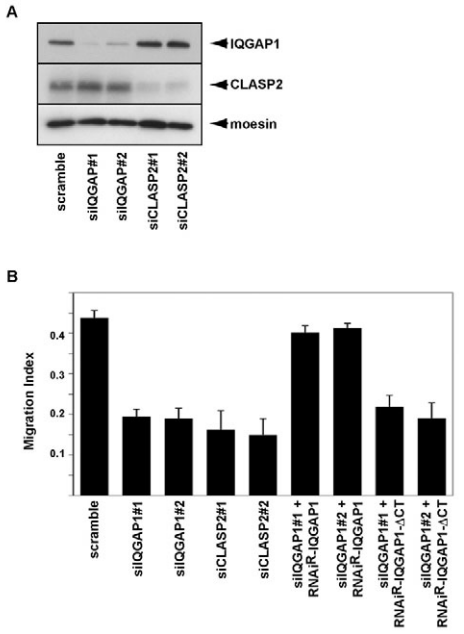

Fig. 8. Requirement of the CLASP2-binding region of IQGAP1 for cell migration. (A) Vero cells were transfected with the indicated siRNA to IQGAP1 or CLASP2. 48 hours after transfection, the lysates were immunoblotted with anti-IQGAP1, anti-CLASP2 and control anti-moesin antibodies. Each siRNA knocked down its target protein. (B) Vero cells transfected with either the indicated siRNA or siRNA along with indicated RNAi^{R}-IQGAP1 were subjected to the Boyden chamber assay. The cells were allowed to migrate for 4 hours. The depletion of either IQGAP1 or CLASP2 significantly impaired cell migration from the upper to the lower membrane. The inhibitory effect of IQGAP1 depletion was rescued by the expression of full-length RNAi^{R}-IQGAP1, but not by expression of RNAi^{R}-IQGAP1-ΔCT lacking the CLASP2-binding region. All results are representative of more than three independent experiments.

phosphorylation, and that nonphosphorylated CLASP2 on microtubules is allowed to associate with IQGAP1 for the coupling of microtubules to actin filaments at the front of migrating cells.

Discussion

Connection of microtubule ends to actin filaments through IQGAP1

Here, we identified IQGAP1, an effector of Rac1 and Cdc42, as a novel CLASP-interacting molecule. IQGAP1 colocalises with actin filaments and partially overlaps with the plus-ends of microtubules at the leading edges of migrating cells (Fukata et al., 2002). We have proposed that activated IQGAP1 captures and stabilises CLIP-170, accumulating only at the plus-ends of microtubules near the specialised cortices such as the leading edges, where it coordinates with APC anchored to actin filaments through IQGAP1 (Watanabe et al., 2005). Consistently, the depletion of IQGAP1 or APC by RNAi prevents not only proper actin meshwork formation, but also stabilisation of the plus-ends of microtubules, which is reflected by the immobilisation of EGFP-CLIP-170 at the leading edges (Watanabe et al., 2004). Since EB1 does not interfere with the binding of IQGAP1 to CLASP2 (supplementary material Fig. S2D), it appears that CLASP2 on the ends of microtubules also participates in the connection to actin filaments through IQGAP1 (Fig. 9). Our recent ultrastructural analysis revealed that IQGAP1 predominantly localises beside actin filaments and at the crossings of actin filaments beneath the substratum-facing plasma membrane (Watanabe et al., 2008). In addition, IQGAP1 sometimes localises to the intersection of microtubule ends and actin filaments. Thus, IQGAP1 appears to be responsible for initial contacts of the plus-ends of microtubules with actin filaments at the leading edges (Fig. 9).

Linkage of CLASP2 to IQGAP1 near microtubule ends

CLASP2 accumulates at the plus-ends of microtubules as well as the lattices behind their plus-ends (Akhmanova et al., 2001; Mimori-Kiyosue et al., 2005; Wittmann and Waterman-Storer, 2005). Since the depletion of IQGAP1 did not affect the localisation of CLASP2 on microtubules (supplementary material Fig. S4), IQGAP1 might not be involved in the process of localisation of CLASP2 to microtubules. We also found that IQGAP1 was cosedimented with polymerised microtubules in the presence but not the absence of CLASP2 (Fig. 5), suggesting that CLASP2 can mediate the interaction of IQGAP1 with microtubules. Of note, IQGAP1 often localises beside microtubules growing along actin filaments beneath the substratum-facing plasma membrane (supplementary material Fig. S4) (Watanabe et al., 2008), suggesting that IQGAP1 can connect CLASP2 to actin filaments not only at the plus-ends of microtubules, but also at the microtubule lattices (Fig. 9). Microtubules and CLASPs consistently undergo retrograde flow with actin filaments in the lamellipodia (Salmon et al., 2002; Tsvetkov et al., 2007; Wittmann and Waterman-Storer, 2001). Thus, the temporal association of IQGAP1 with CLASPs on the ends and lattices of microtubules may have a crucial role in efficient coupling of microtubules in the wider region to actin filaments (Fig. 9).

Possible roles of IQGAP1-mediated cytoskeletal linkages in cell motility

CLASP2 is required for persistent motility, whereas CLIP-170 is not (Akhmanova et al., 2005; Drabek et al., 2006). Truncated APC, lacking the C-terminal region that is responsible for the linkage to microtubules, abrogates polarised migration (Barth et al., 2008; McCartney and Nathke, 2008). We previously reported that the depletion of IQGAP1 or APC impairs cell migration by preventing the proper formation of the actin meshwork (Watanabe et al., 2004). We consistently found that either IQGAP1-depleted or CLASP2-depleted Vero fibroblasts show cell motility defects in the Boyden chamber assay (Fig. 8). The deficiency in the IQGAP1-depleted cells was rescued by the expression of full-length IQGAP1, but not by the expression of IQGAP1-ΔCT. Although IQGAP1-CT includes the binding region for CLASP2, CLIP-170 and APC, the association of IQGAP1 with CLASP2 and/or APC is probably required for cell migration. The interaction of IQGAP1 with CLIP-170 might contribute modestly to cell migration (Fig. 9). However, further analysis will be required to reveal the functional significance of each individual complex in cell motility.

Phosphorylation of CLASP2 by GSK-3β

CLASPs accumulate asymmetrically near the growing plus-ends of microtubules toward the leading edges (Akhmanova et al., 2001; Mimori-Kiyosue et al., 2005; Wittmann and Waterman-Storer, 2005). EB1 is necessary for the recruitment of CLASPs to the plus-ends of microtubules, whereas CLIP-170 is not absolutely required (Mimori-Kiyosue et al., 2005). We found that GSK-3β phosphorylated CLASP2 at Ser533 and Ser537 within the serine/arginine-rich region (Figs 4 and 7). These phosphorylation sites are mapped proximal to the conserved EB1-binding motif

(Galjart, 2005). The expression of active GSK-3β attenuated the binding of CLASP2 to EB1 and abrogated the accumulation of CLASP2 at both the ends and lattices of microtubules (Figs 6 and 7). The middle portion of CLASP2 bound directly to polymerised microtubules in vitro, but the phosphorylated form of CLASP2 did not (Fig. 5). The C-terminal region of CLASPs interacts with CLIP-170 and LL5β (Akhmanova et al., 2001; Lansbergen et al., 2006). Wittmann and Waterman-Storer (Wittmann and Waterman-Storer, 2005) have proposed that the C-terminal region is not involved in the regulation of CLASPs by GSK-3β. Consistent with these observations, GSK-3β did not phosphorylate the C-terminal region of CLASP2 either in vitro or in vivo (Fig. 4; and data not shown). The interaction of CLASPs with CLIP-170 or LL5β might not be controlled by GSK-3β. Collectively, GSK-3β negatively controls the association of CLASP2 with microtubules as well as EB1 through the phosphorylation of CLASP2 at Ser533 and Ser537 for the asymmetrical distribution of CLASPs on microtubules in polarised migrating cells (Fig. 9).

During the course of revision of this paper, Kumar and colleagues (Kumar et al., 2009) published a paper that partially overlaps with this study. They show that a CLASP2 mutant with Ala substitutions at the GSK-3 phosphorylation sites, including the sites we examined, is resistant to the actions of active GSK-3β based on localisation on microtubules. However, phosphomimic mutations impaired binding to polymerised microtubules and EB1 (Kumar et al., 2009). We also show that the CLASP2-2A mutant localises near the ends of microtubules, even in the presence of active GSK-3β (Fig. 6D), whereas phosphorylated CLASP2 does not bind to EB1 and microtubules (Fig. 5B,D). Furthermore, Kumar and co-workers found that expression of active GSK-3β destabilises lamella microtubules by disrupting lateral microtubule interactions with the cell cortex. Since active GSK-3β disrupts complex formation between IQGAP1 and CLASP2 (Fig. 5A), that complex probably contributes to the cytoskeletal linkage at the cell cortex (Fig. 9).

In summary, GSK-3β phosphorylates CLASP2 and controls the asymmetrical distribution of CLASP2 on microtubules. At the leading edges, where GSK-3β is inactivated, nonphosphorylated CLASP2 on microtubules links the microtubules to actin filaments through direct interaction with IQGAP1 for polarised cell migration. IQGAP1 probably has a central role in connecting microtubules to actin filaments, serving as a guiding mechanism through several +TIPs at the leading edge.

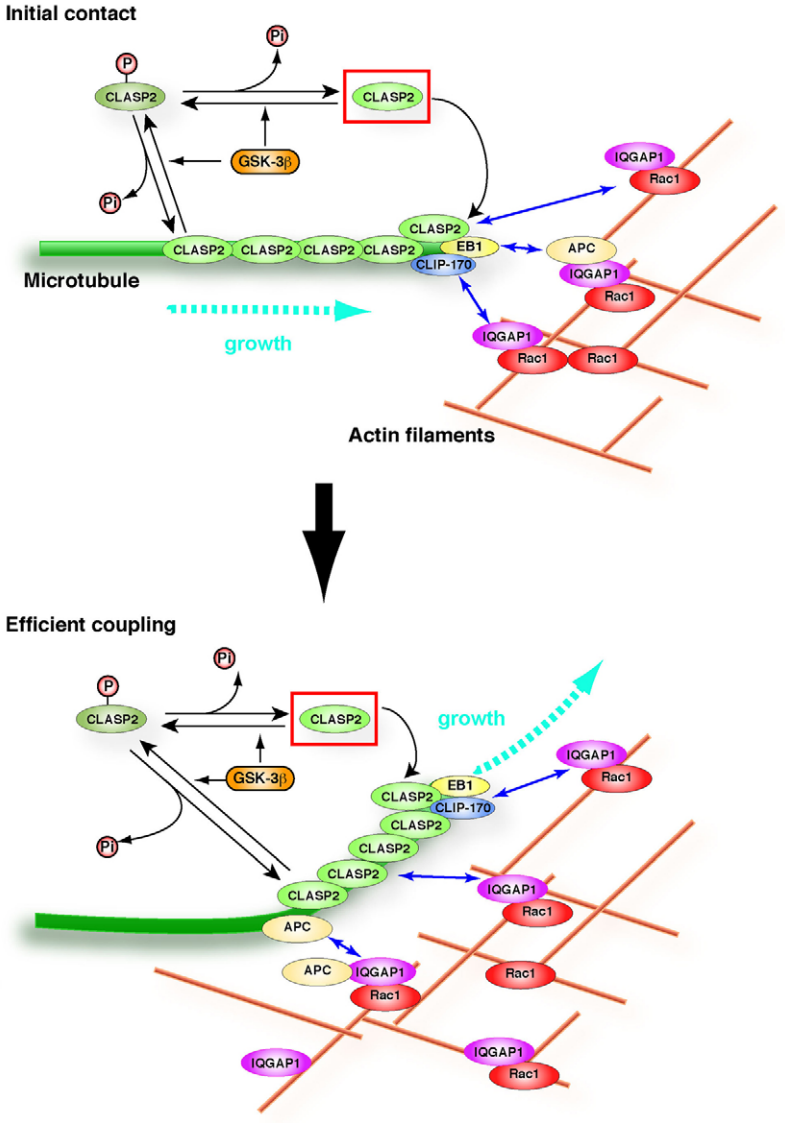

Fig. 9. Regulation of CLASP2 by GSK-3β. A working model summarising the roles of GSK-3β in regulating CLASP activity. At the leading edges of migrating cells, GSK-3β is inactivated, which leads to local accumulation of nonphosphorylated CLASP2 (red box). Nonphosphorylated CLASP2 is able to interact with EB1 and microtubules for asymmetrical distribution in cells. Nonphosphorylated CLASP2 on the ends and lattices of microtubules associates with IQGAP1 for initial contact of microtubules with actin filaments, together with CLIP-170. In addition, CLASP2 on microtubule lattices binds to IQGAP1 for more efficient coupling of microtubules to actin filaments (see text for more detail).

Materials and Methods

Antibodies and reagents

Anti-IQGAP1 monoclonal antibody and anti-GFP antibody were purchased from ZYMED (San Francisco, CA) and Roche (Mannheim, Germany), respectively. pEGFP-C1 was purchased from Clontech Laboratories (Palo Alto, CA). GSK-3 inhibitors (SB216763 and SB415286) were from Tocris Cookson (Ellisville, MO). Recombinant His-tagged Cdk5 and GST-tagged p35 and recombinant His-tagged GSK-3β were from Upstate (Lake Placid, NY). The anti-IQGAP1 rabbit polyclonal antibody has been described elsewhere (Wang et al., 2007). Anti-CLASP2 antibodies were raised against GST-CLASP2-C and produced as described previously (Akhmanova et al., 2001). siRNA sequences are as follows. IQGAP1#1 5′-UGCCAUGGAUGAGAUUGGA-3′; IQGAP1#2 5′-GUUCUACGGGAAGUA-AUUGUU-3′ (designed to 3′UTR region); CLASP2#1 5′-GUUCAGAAAG-CCCUUGAUG-3′; CLASP2#2 5′-GACAUACAUGGGUCUUAGA-3′; scrambled 5′-CAGUCGCGUUUGCGACUGG-3′. These siRNAs with dTdT overhangs at each 3′ terminus were obtained from Greiner-Japan (Tokyo, Japan). siRNA to GSK-3 was purchased from Sigma: GSK-3α#1, SASI_Hs01_00245062; GSK-3α#2, SASI_Hs01_00245062; GSK-3β#1, SASI_Hs01_00192105; GSK-3β#2, SASI_Hs01_00192105. RNAi^{R}-IQGAP1 and its ΔCT were described previously (Watanabe et al., 2004).

Plasmid constructions

To obtain constructs of CLASP2, we defined the KIAA0627 cDNA spanning from position 92 to 3976 (Kazusa DNA Research Institute; Chiba, Japan) as CLASP2, and subcloned the corresponding cDNA fragments into pGEX-4T-1 and pEGFP-C1 vectors. We used the partial KIAA0627 cDNA as CLASP2γ in Fig. 2B. For our amino acid numbering, 533, 537, and 541 correspond to 563, 567, and 571, respectively, in KIAA0627. The constructs of pMal-IQGAP1 fragments and pEF-Bos small GTPases were produced as described elsewhere (Fukata et al., 2002). Tags were fused to the N-termini of proteins of interest. The mutants CLASP2-S533A, -S537A, and -S533A/S537A were generated with a site-directed mutagenesis kit (Stratagene, La Jolla, CA). For microtubule sedimentation assays, the region spanning residues 263 to 581 of CLASP2γ (termed CLASP2-N2-2) was subcloned into the pRSET-C1 vector. Control MBP and MBP-IQGAP1-CT without stop codons were subcloned into the pET52 vector (Merck, Darmstadt, Germany). pCGN-GSK-3β, pCGN-GSK-3β S9A and pCGN-GSK-3β kinase-inactive form (K85N; KN) were provided by Akira Kikuchi (Hiroshima University, Japan).

Preparation of recombinant proteins

The expression and purification of GST and MBP fusion proteins were performed as described (Fukata et al., 2002). For microtubule sedimentation assays, His-CLASP2-N2-2 was purified with Ni-NTA resin according to the manufacturer's protocols (Qiagen, Hilden, Germany). Control MBP and MBP-IQGAP1-CT were purified by sequential passages through two resins, amylose resin and Ni-NTA.

GST-CLASP2-N2 and GST-CLASP2-C affinity column chromatography

The affinity column chromatography was performed as described previously (Kuroda et al., 1996). Briefly, the cytosolic fraction of porcine brain homogenates was loaded onto glutathione Sepharose 4B (GE Healthcare; Little Chalfont, UK) coated with GST alone, GST-CLASP2-N2, or GST-CLASP2-C. The columns were washed with buffer A (20 mM Tris-HCl at pH 8.0, 1 mM dithiothreitol, 1 mM EDTA, 10 mM *p*-amidinophenyl-methanesulfonyl fluoride, and 10 mg/ml leupeptin). The proteins bound to the affinity columns were eluted by buffer A containing 500 mM NaCl and identified as described elsewhere (Fukata et al., 2002).

In vitro binding assays

Purified MBP-fused IQGAP1 fragments were mixed with affinity beads coated with GST-CLASP2-N2 in buffer A. The beads were then washed with buffer A, and the bound proteins were eluted with buffer A containing 10 mM reduced glutathione. The eluates were subjected to SDS-PAGE, followed by immunoblot analysis using an anti-MBP antibody. The amount of IQGAP1-CT bounded with GST-CLASP2-N2 was detected in a linear range using serial dilutions of standards by chemiluminescent detection and estimated with a Densitograph (ATTO, Tokyo, Japan). Purified IQGAP1-CT was used as the standard for quantification.

Cell culture

Vero cells and COS7 cells were grown in Dulbecco's modified Eagle's medium containing 10% foetal bovine serum (FBS) at 37°C in 5% CO_2 atmosphere at constant humidity. Transfection was performed with Lipofectamine 2000 or Lipofectamine (Invitrogen, Carlsbad, CA) according to the manufacturer's protocols. Transfection of siRNA was described previously (Watanabe et al., 2004).

Coimmunoprecipitation of IQGAP1 with CLASP2

The immunoprecipitation assay was performed as described (Fukata et al., 2002). In brief, subconfluent Vero cells or COS7 cells were harvested and lysed with lysis buffer B (20 mM Tris-HCl at pH 7.4, 50 mM NaCl, 10 mM *p*-amidinophenyl-methanesulfonyl fluoride, 10 mg/ml leupeptin, and 0.5% w/v Triton X-100). The lysates were mixed with the indicated antibodies and incubated for 1 hour at 4°C. The immunocomplex was subjected to SDS-PAGE, followed by immunoblotting with the indicated antibodies.

Kinase assay

The kinase reaction for His-GSK-3β was carried out in 50 μl kinase buffer (50 mM Tris-HCl at pH 7.5, 5 mM $MgCl_2$, 0.3 mM dithiothreitol) containing 100 μM [γ-^{32}P]ATP, recombinant kinases (20 ng His-GSK-3β and/or 10 ng His-Cdk5 with GST-p35), and substrate (1 μM GST-CLASP2 protein). After incubation for 30 minutes at 30°C, the reaction mixtures were boiled in SDS sample buffer and subjected to SDS-PAGE and silver staining. The radiolabelled bands were visualised with an image analyser (BAS1500; Fuji, Tokyo, Japan).

Purification and preparation of anti-S533/S537-*P* antibody

A rabbit polyclonal antibody against CLASP2 phosphorylated at Ser533 and Ser537 (anti-S533/S537-*P* antibody) was raised as described previously (Amano et al., 2003). The phosphopeptide Cys528-Ser-Arg-Glu-Ala-Ser533(-*P*)-Arg-Glu-Ser-Ser537(-*P*)-Arg-Asp-Thr-Ser-Pro542 was chemically synthesised by Biologica (Aichi, Japan) as an antigen for CLASP2. The antiserum obtained was then affinity-purified against the respective phosphopeptide.

Microtubule sedimentation assays

The microtubule sedimentation assays was performed with purified proteins as described previously (Fukata et al., 2002). Porcine tubulin was obtained from Cytoskeleton (Denver, CO).

Boyden chamber assay

siRNA was transfected into Vero cells with either GFP-GST or RNAi^{R}-IQGAP1. Cell migration assays were performed using Transwell plates (pore size of 8 μm; HTS FluoroBlok Insert; Becton Dickinson, Franklin Lakes, NJ). The undersurface of the membrane was coated with 10 μg/ml fibronectin (Becton Dickinson) diluted in distilled water at room temperature for 1 hour. The cells were seeded in the upper chamber (1×10^4 per well) in 500 μl DMEM with 0.1% bovine serum albumin (BSA). DMEM supplemented with 0.1% BSA and 10% FBS was added into the lower chamber. The cells were allowed to migrate for 4 hours. After fixation, both nonmigrated and migrated EGFP-positive cells were counted by EGFP fluorescence. The ratio of migrated cells to total (migrated + nonmigrated) cells was calculated. At least 300 EGFP-positive cells were counted in each group for each experiment. The results were normalised and expressed as a migration index.

Immunofluorescence analysis

For visualisation of +TIPs and microtubules, the cells were fixed with cold methanol containing 1 mM EGTA for 20 minutes at –20°C. When necessary, the cells were postfixed with 3.7% formaldehyde in PBS for 10 minutes and permeabilised with PBS containing 0.2% Triton X-100 and 1 mg/ml BSA for an additional 10 minutes. The cells were then stained with the indicated primary antibodies. Cy2-, Cy3-, and Cy5-conjugated secondary antibodies (Jackson ImmunoResearch Laboratories, West Grove, PA) were used for immunofluorescence analysis. Fluorescence was examined using a confocal laser-scanning microscope (Carl Zeiss LSM 510; Carl Zeiss, Oberkochene, Germany) built around a Zeiss Axio-vert 100M with Plan-APOCHROMAT (63× NA 1.4 Oil). The images were acquired and processed by LSM software (Carl Zeiss).

We thank Eisuke Mekada (Osaka University, Japan) for providing the Vero cells, Akira Kikuchi (Hiroshima University, Japan) for providing the GSK-3β constructs, and Akira Okamoto (Nagoya University, Japan) for helpful technical support. We also thank all members of the Kaibuchi laboratory, especially Mutsuki Amano, Masaki Fukata, and Yuko Fukata (National Institute for Physiological Sciences) for helpful discussions, and Kiyoko Murase, Sumi Kamisawa, Sachi Kozawa, and Takako Ishii for technical and secretarial assistance. This research was supported in part by Special Coordination Funds for Promoting Science and Technology (SCF), a Grant-in-Aid for Scientific Research, the Human Frontier Science Program (HFSP), a Grant-in-Aid for Creative Scientific Research (JSPS), a Grant-in-Aid for JSPS Fellows (JSPS), the 21st Century Centre of Excellence (COE) Program from MEXT, the Global COE Program from MEXT, and the Grant-in-Aid for CREST (JST). N.G. was supported by grants from the Netherlands Organisation for Scientific Research (NWO-ALW and NWO-MW), the Netherlands Ministry of Economic Affairs (BSIK) and the Dutch Cancer Society (KWF).

References

Akhmanova, A. and Steinmetz, M. O. (2008). Tracking the ends: a dynamic protein network controls the fate of microtubule tips. *Nat. Rev. Mol. Cell Biol.* **9**, 309-322.

Akhmanova, A., Hoogenraad, C. C., Drabek, K., Stepanova, T., Dortland, B., Verkerk, T., Vermeulen, W., Burgering, B. M., De Zeeuw, C. I., Grosveld, F. et al. (2001). Clasps are CLIP-115 and -170 associating proteins involved in the regional regulation of microtubule dynamics in motile fibroblasts. *Cell* **104**, 923-935.

Akhmanova, A., Mausset-Bonnefont, A. L., van Cappellen, W., Keijzer, N., Hoogenraad, C. C., Stepanova, T., Drabek, K., van der Wees, J., Mommaas, M., Onderwater, J. et al. (2005). The microtubule plus-end-tracking protein CLIP-170 associates with the spermatid manchette and is essential for spermatogenesis. *Genes Dev.* **19**, 2501-2515.

Amano, M., Kaneko, T., Maeda, A., Nakayama, M., Ito, M., Yamauchi, T., Goto, H., Fukata, Y., Oshiro, N., Shinohara, A. et al. (2003). Identification of Tau and MAP2 as novel substrates of Rho-kinase and myosin phosphatase. *J. Neurochem.* **87**, 780-790.

Barth, A. I., Caro-Gonzalez, H. Y. and Nelson, W. J. (2008). Role of adenomatous polyposis coli (APC) and microtubules in directional cell migration and neuronal polarization. *Semin. Cell Dev. Biol.* **19**, 245-251.

Bienz, M. (2002). The subcellular destinations of APC proteins. *Nat. Rev. Mol. Cell Biol.* **3**, 328-338.

Burridge, K. and Wennerberg, K. (2004). Rho and Rac take center stage. *Cell* **116**, 167-179.

Cohen, P. and Frame, S. (2001). The renaissance of GSK3. *Nat. Rev. Mol. Cell Biol.* **2**, 769-776.

Drabek, K., van Ham, M., Stepanova, T., Draegestein, K., van Horssen, R., Sayas, C. L., Akhmanova, A., Ten Hagen, T., Smits, R., Fodde, R. et al. (2006). Role of CLASP2 in microtubule stabilization and the regulation of persistent motility. *Curr. Biol.* **16**, 2259-2264.

Eldar-Finkelman, H. (2002). Glycogen synthase kinase **3**, an emerging therapeutic target. *Trends Mol. Med.* **8**, 126-132.

Etienne-Manneville, S. (2004). Cdc42-the centre of polarity. *J. Cell Sci.* **117**, 1291-1300.

Etienne-Manneville, S. and Hall, A. (2003). Cdc42 regulates GSK-3beta and adenomatous polyposis coli to control cell polarity. *Nature* **421**, 753-756.

Fukata, M., Watanabe, T., Noritake, J., Nakagawa, M., Yamaga, M., Kuroda, S., Matsuura, Y., Iwamatsu, A., Perez, F. and Kaibuchi, K. (2002). Rac1 and Cdc42 capture microtubules through IQGAP1 and CLIP-170. *Cell* **109**, 873-885.

Fukata, M., Nakagawa, M. and Kaibuchi, K. (2003). Roles of Rho-family GTPases in cell polarisation and directional migration. *Curr. Opin. Cell Biol.* **15**, 590-597.

Galjart, N. (2005). CLIPs and CLASPs and cellular dynamics. *Nat. Rev. Mol. Cell Biol.* **6**, 487-498.

Gundersen, G. G., Gomes, E. R. and Wen, Y. (2004). Cortical control of microtubule stability and polarization. *Curr. Opin. Cell Biol.* **16**, 106-112.

Hart, M. J., Callow, M. G., Souza, B. and Polakis, P. (1996). IQGAP1, a calmodulin-binding protein with a rasGAP-related domain, is a potential effector for cdc42Hs. *EMBO J.* **15**, 2997-3005.

Jaffe, A. B. and Hall, A. (2005). Rho GTPases: biochemistry and biology. *Annu. Rev. Cell Dev. Biol.* **21**, 247-269.

Kirschner, M. and Mitchison, T. (1986). Beyond self-assembly: from microtubules to morphogenesis. *Cell* **45**, 329-342.

Kumar, P., Lyle, K. S., Gierke, S., Matov, A., Danuser, G. and Wittmann, T. (2009). GSK3β phosphorylation modulates CLASP-microtubule association and lamella microtubule attachment. *J. Cell Biol.* **184**, 895-908.

Kuroda, S., Fukata, M., Kobayashi, K., Nakafuku, M., Nomura, N., Iwamatsu, A. and Kaibuchi, K. (1996). Identification of IQGAP as a putative target for the small GTPases, Cdc42 and Rac1. *J. Biol. Chem.* **271**, 23363-23367.

Lansbergen, G., Grigoriev, I., Mimori-Kiyosue, Y., Ohtsuka, T., Higa, S., Kitajima, I., Demmers, J., Galjart, N., Houtsmuller, A. B., Grosveld, F. et al. (2006). CLASPs attach microtubule plus ends to the cell cortex through a complex with LL5beta. *Dev. Cell* **11**, 21-32.

McCallum, S. J., Wu, W. J. and Cerione, R. A. (1996). Identification of a putative effector for Cdc42Hs with high sequence similarity to the RasGAP-related protein IQGAP1 and a Cdc42Hs binding partner with similarity to IQGAP2. *J. Biol. Chem.* **271**, 21732-21737.

McCartney, B. M. and Nathke, I. S. (2008). Cell regulation by the Apc protein Apc as master regulator of epithelia. *Curr. Opin. Cell Biol.* **20**, 186-193.

Mimori-Kiyosue, Y., Grigoriev, I., Lansbergen, G., Sasaki, H., Matsui, C., Severin, F., Galjart, N., Grosveld, F., Vorobjev, I., Tsukita, S. et al. (2005). CLASP1 and CLASP2 bind to EB1 and regulate microtubule plus-end dynamics at the cell cortex. *J. Cell Biol.* **168**, 141-153.

Nathke, I. S., Adams, C. L., Polakis, P., Sellin, J. H. and Nelson, W. J. (1996). The adenomatous polyposis coli tumor suppressor protein localizes to plasma membrane sites involved in active cell migration. *J. Cell Biol.* **134**, 165-179.

Reilein, A. and Nelson, W. J. (2005). APC is a component of an organizing template for cortical microtubule networks. *Nat. Cell Biol.* **7**, 463-473.

Ridley, A. J., Schwartz, M. A., Burridge, K., Firtel, R. A., Ginsberg, M. H., Borisy, G., Parsons, J. T. and Horwitz, A. R. (2003). Cell migration: integrating signals from front to back. *Science* **302**, 1704-1709.

Rodriguez, O. C., Schaefer, A. W., Mandato, C. A., Forscher, P., Bement, W. M. and Waterman-Storer, C. M. (2003). Conserved microtubule-actin interactions in cell movement and morphogenesis. *Nat. Cell Biol.* **5**, 599-609.

Salmon, W. C., Adams, M. C. and Waterman-Storer, C. M. (2002). Dual-wavelength fluorescent speckle microscopy reveals coupling of microtubule and actin movements in migrating cells. *J. Cell Biol.* **158**, 31-37.

Tsvetkov, A. S., Samsonov, A., Akhmanova, A., Galjart, N. and Popov, S. V. (2007). Microtubule-binding proteins CLASP1 and CLASP2 interact with actin filaments. *Cell Motil. Cytoskeleton* **64**, 519-530.

Wang, S., Watanabe, T., Noritake, J., Fukata, M., Yoshimura, T., Itoh, N., Harada, T., Nakagawa, M., Matsuura, Y., Arimura, N. et al. (2007). IQGAP3, a novel effector of Rac1 and Cdc42, regulates neurite outgrowth. *J. Cell Sci.* **120**, 567-577.

Watanabe, T., Wang, S., Noritake, J., Sato, K., Fukata, M., Takefuji, M., Nakagawa, M., Izumi, N., Akiyama, T. and Kaibuchi, K. (2004). Interaction with IQGAP1 links APC to Rac1, Cdc42, and actin filaments during cell polarization and migration. *Dev. Cell* **7**, 871-883.

Watanabe, T., Noritake, J. and Kaibuchi, K. (2005). Regulation of microtubules in cell migration. *Trends Cell Biol.* **15**, 76-83.

Watanabe, T., Wang, S., Kakeno, M., Usukura, J. and Kaibuchi, K. (2008). Ultrastructural study of Rac1 and its effectors beneath the substratum-facing membrane. *Cell Struct. Funct.* **33**, 101-107.

Wittmann, T. and Waterman-Storer, C. M. (2001). Cell motility: can Rho GTPases and microtubules point the way? *J. Cell Sci.* **114**, 3795-3803.

Wittmann, T. and Waterman-Storer, C. M. (2005). Spatial regulation of CLASP affinity for microtubules by Rac1 and GSK3beta in migrating epithelial cells. *J. Cell Biol.* **169**, 929-939.

Zumbrunn, J., Kinoshita, K., Hyman, A. A. and Nathke, I. S. (2001). Binding of the adenomatous polyposis coli protein to microtubules increases microtubule stability and is regulated by GSK3 beta phosphorylation. *Curr. Biol.* **11**, 44-49.